Fig. 3 shows the output spectra of the array for various driving currents, where care has been taken that all lasing modes are collected by the spectrometer. The transverse multimode spectral profile very much resembles that of a single lasing element in the array. The 10dB down spectral width is < 2nm. The red shift of the spectrum with dissipated power amounts to 0.002nm/mW. The far field of the array is single-lobed with a 3dB full width divergence angle of ~12°. The near field pattern consists of nine rather homogeneous bright circles that radiate on a multitude of transverse modes.

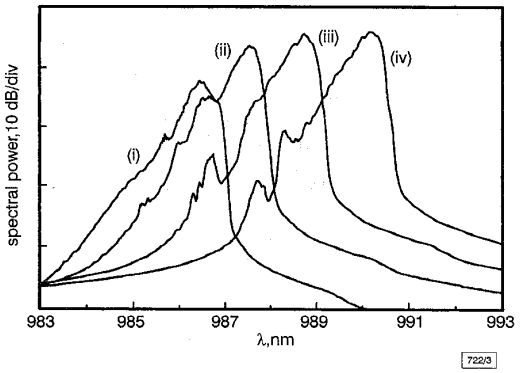

Fig. 3 *Array output spectra for various driving currents*

(i) I = 250mA
(ii) I = 500mA
(iii) I = 750mA
(iv) I = 1000mA

Thermal crosstalk is considered to have a strong influence on the characteristics of densely packed VCSEL arrays. Therefore, heat sinking of the array is crucial for reduction of both thermal resistance and thermal crosstalk. We define thermal crosstalk as a temperature increase of an individual lasing element in the array, due to the influence of the heat dissipation of a neighbouring element. Measurements are carried out, observing the modal wavelength shift of one element driven under pulsed conditions and controlled heat dissipation from another VCSEL running CW. For the studied 140μm pitch 3 × 3 array we have measured thermal crosstalks of 100 and 30K/W for the shortest (140μm) and the longest (396μm) distance between unmounted individual elements, respectively. Comparing these figures with the thermal resistance of 250K/W measured for single unmounted 50μm size VCSELs shows that thermal crosstalk does very much determine array operation, and stresses the importance of efficient heat dissipation in high power VCSEL arrays. With our mounting technique the thermal resistance of the heat sunk array is reduced approximately by a factor of 5. Since threshold current densities remain the same before and after mounting, and no significant inhomogeneities in the near field intensity profiles across all nine elements are observed even near thermal rollover, thermal crosstalk is considered negligibly small after mounting of the array.

Summary: We have fabricated 140μm pitch 3 × 3 VCSEL arrays that achieve 650mW optical output power at corresponding 15% power conversion efficiency and 370W/cm² spatially averaged near field power density. Maximum conversion efficiency is 25% at 270mW output power. The 10 dB down spectral width is < 2nm, and the full width 3dB beam divergence is < 12°. Analysis shows that efficient heat sinking is important to reduce thermal resistance and crosstalk in high power arrays.

Acknowledgments: Support by the German Ministry of Research and Technology (BMBF) is gratefully acknowledged.

4 May 1998
Electronics Letters Online No: 19980842

M. Grabherr, M. Miller, R. Jäger and K.J. Ebeling (*Department of Optoelectronics, University of Ulm, Albert-Einstein-Allee 45, 89069 Ulm, Germany*)

E-mail: martin.grabherr@e-technik.uni-ulm.de

References

1 JÄGER, R., GRABHERR, M., JUNG, C., MICHALZIK, R., REINER, G., WEIGL, B., and EBELING, K.J.: '57% wallpiug efficiency oxide-confined 850nm wavelength GaAs VCSELs', *Electron. Lett.*, 1997, **33**, pp. 330–331

2 LEAR, K.L., CHOQUETTE, K.D., SCHNEIDER, R.P., KILCOYNE, S.P., and GEIB, K.M.: 'Selectively oxidised vertical-cavity surface-emitting lasers with 50% power conversion efficiency', *Electron. Lett.*, 1995, **31**, pp. 208–209

3 WEIGL, B., GRABHERR, M., JUNG, C., JÄGER, R., REINER, G., MICHALZIK, R., SOWADA, D., and EBELING, K.J.: 'High-performance oxide-confined GaAs VCSELs', *IEEE J. Sel. Top. Quantum Electron.*, 1997, **3**, pp. 409–415

4 GRABHERR, M., WEIGL, B., REINER, G., MILLER, M., and EBELING, K.J.: 'High power top-surface emitting oxide confined vertical-cavity lasers', *Electron. Lett.*, 1996, **32**, pp. 1723–1724

5 PETERS, F.H., PETERS, M.G., YOUNG, D.B., SCOTT, J.W., THIBEAULT, B,J., CORZINE, S.W, and COLDREN, L.A.: 'High power vertical-cavity surface-emitting lasers', *Electron. Lett.*, 1993, **29**, pp. 200–201

6 GRABHERR, M., JÄGER, R., MILLER, M., THALMAIER, C., HEERLEIN, J., MICHALZIK, R., and EBELING, K.J.: 'Bottom emitting VCSELs for high CW optical output power', submitted to *IEEE Photonics Technol. Lett.*, 1998

7 CHOQUETTE, K.D., HOU, H.Q., GEIB, K.M., and HAMMONS, B.E.: 'Uniform and high power selectively oxidized 8 × 8 VCSEL array'. LEOS Summer Topical Meetings, Montreal, Canada, 1997, Paper MB2

8 GRAYDON, O.: 'High-power diodes seal, strip and engrave', *Opto Laser Eur.*, 1997, **45**, pp. 23–25

Efficient Q-switched Ti:Er:$LiNbO_3$ waveguide laser

H. Suche, T. Oesselke, J. Pandavenes, R. Ricken, K. Rochhausen, W. Sohler, S. Balsamo, I. Montrosset and K.K. Wong

Diode-pumped Q-switched Ti:Er:$LiNbO_3$ waveguide lasers have been developed with a monolithically integrated folded Mach-Zehnder type modulator of high extinction ratio as the Q-switch. The lasers are operated at 1562nm wavelength, emitting pulses of 4.3ns halfwidth with up to 1.44kW peak power at 1kHz repetition frequency. Good agreement between experimental and theoretical results has been obtained.

Introduction: Diode-pumped integrated Q-switched lasers can be efficient, miniaturised sources of short optical pulses with a variety of possible applications. They could be used as pump sources for parametric nonlinear frequency conversion, as sources for optical time domain reflectometry (OTDR) and for light detection and ranging (LIDAR). For the latter application, eye-safe sources are frequently recommended. Er-doped Q-switched lasers emitting at ~1.55μm wavelength meet this requirement and have therefore attracted increasing attention in recent years [1 – 3]. Among the different possible substrates for Er-doped waveguide lasers, $LiNbO_3$ is very attractive. High concentrations of Er up to the solid solubility limit can be achieved by indiffusion without significant fluorescence quenching. This feature, together with the long fluorescence lifetime of the Er ions, guarantees a high energy storage capability and a high power conversion efficiency which can be exploited for the design of efficient Q-switched waveguide lasers. Peak power levels in the kilowatt range have been predicted [3]. Moreover, owing to the excellent electro-optic properties of the $LiNbO_3$ substrate, the required intracavity switch can be monolithically integrated [4] leading to a compact and rugged laser design. Recently, we reported the first monolithic Q-switched Ti:Er:$LiNbO_3$ waveguide laser using a folded Mach-Zehnder intensity modulator with a directional coupler as the Q-switch [1, 5]. However, the laser performance (2.4W peak power, 180nJ pulse energy at 2kHz repetition rate) was limited by the onset of prelasing because of the poor loss modulation characteristics of the switch.

In this Letter we present the first results of a drastically improved Q-switched laser with up to 1.44kW peak power using a modified switch with high extinction ratio.

Design and fabrication: In Fig. 1 a schematic drawing of the structure of the Q-switched laser and the experimental setup are shown. The laser utilises a folded intracavity Mach-Zehnder (MZ) type intensity modulator as the Q-switch. The pump radiation is launched into the waveguide cavity by a fibre optic wavelength division multiplexer (WDM) and the Q-switched laser emission is extracted in the backward direction.

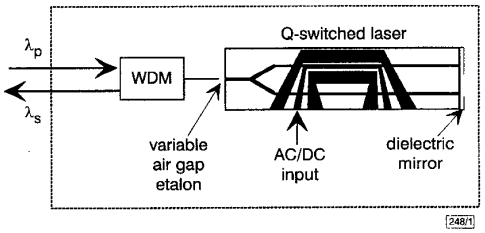

Fig. 1 *Schematic drawing of laser structure and experimental setup for investigation of Q-switched laser operation*

The actual device has a length of ~75mm. Half (with respect to the X-direction) of the Z-cut (Y-propagation) $LiNbO_3$ substrate has been doped over its complete length near the surface by indiffusion of 30nm of vacuum deposited Er at 1130°C over 150h. Subsequently, the photolithographically delineated 7μm wide and 100nm thick structure of Ti-stripes has been indiffused at 1060°C over 7.5h to form the waveguide channels. In the undoped region, waveguide scattering losses of 0.03dB/cm have been measured. The splitter is a Y-junction with X-sine shaped bends located in the centre of the cavity. Its excess loss is ~0.15dB and its deviation from symmetrical power splitting is < 0.2dB, leading to an estimated modulator extinction ratio of better than –25dB. On the waveguide structure a 0.6μm thick insulating SiO_2 buffer has been vacuum deposited prior to the electrode fabrication.

The electrode structure of the intracavity modulator (Q-switch) is a 25mm long symmetrical coplanar microstrip line fabricated by lift-off of a sandwich of sputtered Ti/Au. The modulator has been operated as a lumped device without low resistance termination due to the relaxed bandwidth requirements. The halfwave voltage for the laser polarisation TE- (σ-) is ~28V owing to the smaller electro-optic coefficient available in this polarisation.

The laser has a Fabry Perot cavity comprised of a dielectric mirror vacuum deposited on the polished waveguide endfaces and a variable etalon with an air gap. The dielectric mirror has a high reflectance (98%) at both the emission wavelength ($\lambda_s \simeq$ 1562nm, σ-polarised or $\lambda_s \simeq$ 1575nm, π-polarised) and the pump wavelength ($\lambda_p \simeq$ 1480nm). Hence, double pass pumping is provided, allowing an improved pump absorption efficiency. On the other side a variable output/pump coupler mirror has been realised by an adjustable, piezoelectrically driven air gap etalon formed by the endfaces of the pump input/signal output fibre (common branch) of the WDM and the polished Ti:Er:$LiNbO_3$ waveguide endface. The effective reflectance of this mirror can be adjusted in the range $0.03 < R < 0.3$.

Experimental and theoretical results: Using a pigtailed laser diode ($\lambda_p \simeq$ 1480nm) of up to 145mW output power as the pump source, a threshold of ~90mW (σ-polarised) has been achieved for σ-polarised emission at 1562nm wavelength. The modulator has been operated with a DC-bias voltage to give maximum optical extinction and an AC-switching voltage (square wave) of amplitude $V\pi$ and ~5% duty cycle in the frequency range 1–10kHz. No evidence of prelasing could be identified. The Q-switched pulses have been attenuated by 50dB in a cascade of fibre optic splitters and attenuators to ensure linearity of the detector, a biased *pin* photodiode of 1.5GHz bandwidth. The detector signal has been measured using a scope of 1.5GHz bandwidth.

A numerical code has been developed to simulate the dynamic behaviour of such a laser, based on the following hypothesis:

(i) The Er:$LiNbO_3$ system has been approximated as a quasi-two level system.

(ii) The multi-longitudinal mode laser cavity and the pump dynamics have been represented with the mean field approximation.

(iii) Three different rate equations have been used to approximate the population inversion in the different parts of the folded MZ cavity.

The system of N_{mode} + 4 coupled nonlinear differential equations has been solved numerically [5] with an adaptive time-step routine suitable for stiff systems.

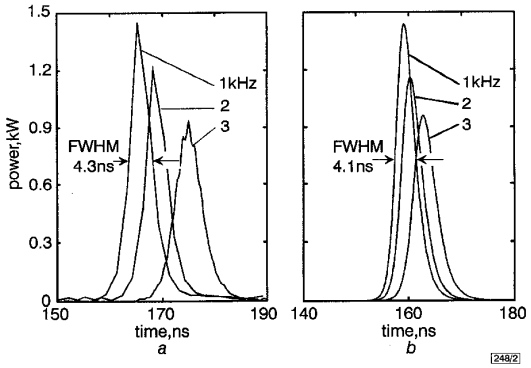

Fig. 2 *Output power of Q-switched Ti:Er: $LiNbO_3$ waveguide laser against time*

a Measured through pump/output coupler in backward direction; zero of abscissa scale coincides with leading edge of electrical switching pulse; parameter of graphs is pulse repetition frequency
b Numerically simulated results for comparison

In Fig. 2 the experimental and theoretical results of Q-switched operation of the Ti:Er:$LiNbO_3$ waveguide laser are presented for 145mW incident pump power. The zero point of the abscissa of the diagrams corresponds to the leading edge of the electrical switching pulse. At 1kHz repetition rate, up to 1.44kW peak power has been measured. The build up time is ~165ns and the pulsewidth is 4.3ns (FWHM). With increasing repetition rate the peak power degrades and the pulsewidth and build-up time increase, respectively.

Good agreement between measured and calculated peak power levels and pulsewidths has been achieved.

We also investigated the output spectrum emitted from both endfaces of the waveguide laser. At the maximum pump power level, the spectrum emitted from the high reflector side of the cavity is 40 times narrower (*FWHM* = 2.5nm) than the spectrum emitted in the backward direction through the pump coupler and the cascade of fibre components. We attribute this to the generation of Raman shifted light in the fibre. As a result, part of the optical power is shifted to longer wavelengths where the detector sensitivity is reduced. Therefore, with increasing pump power the ratio of the dectected peak power levels emitted in the forward and backward directions is increased by a factor of 1.3. For that reason, in Fig. 2*a* the maximum peak power level has to be corrected, i.e. multiplied, by this factor.

For π-polarised pumping, π-polarised emission at 1575nm has been observed with significantly lower peak powers (up to ~500W) compared to the σ-polarised emission at 1562nm wavelength.

Conclusion: We report the first Q-switched Ti:Er:$LiNbO_3$ waveguide laser emitting pulses of 4.3ns width and > 1.4kW peak power at 1kHz repetition frequency with only 145mW of continuous wave pump power. Good agreement between measured and simulated results has been achieved. A laser of this type has already been pigtailed and packaged. It will be tested for LIDAR-applications in the near future.

5 May 1998
Electronics Letters Online No: 19980888

H. Suche, T. Oesselke, J. Pandavenes, R. Ricken, K. Rochhausen and W. Sohler (*Universität-GH Paderborn, Angewandte Physik, Warburger Straße 100, D-33098 Paderborn, Germany*)

E-mail: suche@physik.uni-paderborn.de

S. Balsamo and I. Montrosset (*Politecnico di Torino, Dipartimento de Elettronica, Corso Duca Degli Abruzzi 24, I-10129 Torino, Italy*)

K.K. Wong (*IMRA America, Inc., 1044 Woodridge Avenue, Ann Arbor, MI 48105-9774, USA*)

References

1 BAUMANN, I., BOSSO, S., BRINKMANN, R., CORSINI, R., DINAND, M., GREINER, A., SCHÄFER, K., SÖCHTIG, J., SOHLER, W., SUCHE, H., and WESSEL, R.: 'Er-doped integrated optical devices in $LiNbO_3$', *IEEE J. Sel. Topics Quantum Electron.*, 1996, **2**, (2), pp. 355–366

2 YENIAY, A., DELAVAUX, J.-M.P., TOULOUSE, J., BARBIER, D., STRASSER, T.A., PEDRAZANNI, J.R., and MINFORD, W.: 'Hybrid Q-switched laser with Ti-indiffused $LiNbO_3$ and Er-Yb codoped glass waveguides', *IEEE Photonics Technol. Lett.*, 1997, **9**, (12), pp. 1580–1582

3 VEASEY, D.L., GARY, J.M., AMIN, J., and AUST, J.A.: 'Time-dependent modelling of erbium-doped waveguide lasers in lithium niobate pumped at 980 and 1480nm', *IEEE J. Quantum Electron.*, 1997, **33**, (10), pp. 1647–1662

4 LALLIER, E., PAPILLON, D., POCHOLLE, J.P., PAPUCHON, M., DE MICHELI, M., and OSTROWSKY, D.B.: 'Short pulse, high power Q-switched Nd:MgO:$LiNbO_3$ waveguide laser', *Electron. Lett.*, 1993, **29**, (2), pp. 175–176

5 BALSAMO, S., MAIO, S., MONTROSSET, I., SUCHE, H., and SOHLER, W.: 'Q-switched Ti:Er:$LiNbO_3$ waveguide laser' (submitted for publication)

Experimental evidence of nonuniform carrier distribution in multiple-quantum-well laser diodes

Bor-Lin Lee, Ching-Fuh Lin, Jie-Wei Lai and Wei Lin

Carrier distribution in multiple quantum wells is studied. Nonuniform carrier distribution is evidenced by the lasing characteristics of laser diodes with multiple quantum wells of different widths. It is shown that the well sequence significantly influences the threshold current and the characteristic temperature owing to nonuniform carrier distribution.

Carrier distribution in multiple quantum wells (MQWs) is an important issue for understanding the static and dynamic behaviour of QWs [1]. The carrier distribution over MQWs is highly nonuniform and has been studied theoretically [2, 3]. In contrast, less experimental evidence has been presented [4]. In this Letter, we demonstrate the experimental evidence of nonuniform carrier distribution by measuring the lasing characteristics of laser diodes fabricated on substrates with four quantum wells of different widths.

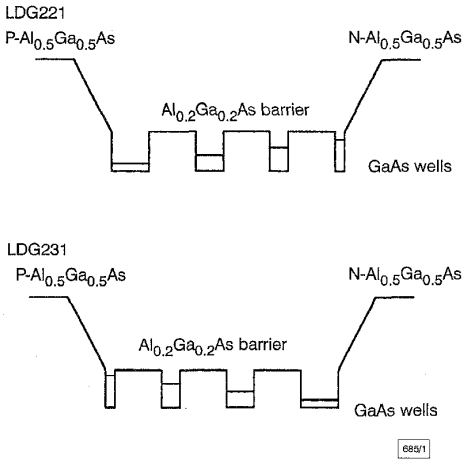

Fig. 1 *Layer structures of four quantum wells of different widths*

The layer structures of the substrates with four quantum wells for the study are shown schematically in Fig. 1. The well widths are 20, 33, 56, and 125Å, respectively. Their $n = 1$ transitions separate for ~50meV, which is large enough to distinguish the corresponding emission spectra. Therefore, the spectrum measurement can be used to identify which well contributes to the emission. Two different sequences of the four wells have been grown by MOCVD. They are termed LDG221 and LDG231, and their sequences are shown in Fig. 1. The LDG231 sample has been used to fabricate superluminescent diodes which demonstrate that all four wells are able to contribute significant emission [5]. Standard processing techniques were used for the device fabrication. Fabry-Perot laser diodes with a 6 μm ridge waveguide were fabricated on the two types of substrate. No coatings were applied to the device facets. The measured devices are all 700μm long.

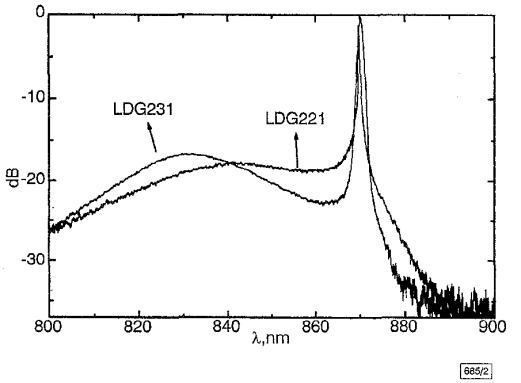

Fig. 2 *Measured spectra of laser diodes*

Fig. 2 shows the measured spectra of the fabricated Fabry-Perot laser diodes. The variation of the lasing wavelength with temperature is also shown in Table 1. In spite of the different sequences of the four wells, they both oscillate at the wavelength around 870 nm, which corresponds to the emission energy of the 125Å well. Because emissions due to the narrow wells always have a larger energy than the separation energy of the first quantised states in the conduction and the valence bands of the widest well, they could be absorbed by the widest well. Consequently, the emission of the widest well experiences the least loss and oscillation is most likely to occur at the corresponding transition wavelength.

Table 1: Variation of lasing wavelength with temperature

λ	LDG221	LDG231
°C		
20	867.3	867.5
30	869.7	870.5
40	871.8	873.3
50	874.8	875.7

Although the emission wavelength is the same, the threshold currents of the laser diodes fabricated from the two samples are different. Those fabricated on the LDG221 substrate have a threshold current ~30mA, while those fabricated on the LDG231 substrate have a threshold current almost twice this. The reason for this is discussed briefly in the following. The threshold current of a laser diode is determined by its material gain, confinement factor, internal loss, and mirror loss. Because the two samples have the same separate confinement heterostructures and waveguide structures, their internal loss, mirror loss, and confinement factor are approximately the same. This indicates that the difference in threshold comes from the different material gain at the same injection condition. The material gain depends on temperature, well/barrier structure, and carrier density in the QW [6]. Therefore, we believe that the carrier distribution among the four wells is different for the two samples. Because the LDG221 sample has its 125Å well closest to the *p*-cladding layer, it has more holes accumulated in this wide well than the LDG231 sample has at the same injection current. Conversely, the LDG231 sample has the 125Å well closest to the *n*-cladding layer, so it has more electrons accumulated in this well than does the LDG221 sample. The experimental measurements indicate that the distribution of holes is the dominant factor. As a result, with the same injected current, LDG221 devices have more gain for the wavelength corresponding to the 125Å well than do the LDG231 devices, leading to a significantly reduced threshold current for the LDG221 devices.